Available online at www.sciencedirect.com

ScienceDirect

Energy Procedia 35 (2013) 2 – 11

Energy Procedia

DeepWind'2013, 24-25 January, Trondheim, Norway

Geometric scaling effects of bend-twist coupling in rotor blades

Kevin Cox[a]*, Andreas Echtermeyer[a]

[a]*Dept. of Engineering Design and Materials, Norwegian University of Science and Technology, Richard Birkelandsvei 2B, Trondheim 7491, Norway*

Abstract

Blade lengths of 30, 50, 70 and 90m were designed to quantify the effect of geometric scaling on bend-twist coupling. The blades were implemented with off-axis carbon fibers in the spar flanges to promote coupling while biaxial glass fibers were used to provide torsional stiffness and buckling resistance. Theoretical scaling laws were compared to nonlinear finite element simulations, both of which concluded that there was no dependence of bend-twist coupling on geometric up-scaling. At the maximum load, all blades achieved a tip twist between 6 and 7° towards feather. This resulted in load reductions of roughly 10-11%, showing that load alleviation from bend-twist coupling was also independent of scaling effects. The reduction in loads showed potential for blade mass reduction.

Keywords: wind turbine blade; unbalanced composite layup; adaptive blade; up-scaling; FEA

1. Introduction

The migration of wind turbines from land based to offshore installations is being pursued in hope of achieving a lower cost of energy. Offshore installations allow for larger turbines and the wind speed is generally faster and steadier there than at many onshore locations. Typical offshore turbine designs incorporate a variable speed rotor, a variable pitch control system, and 3 long glass/carbon fiber composite blades oriented upwind of the tower. As wind turbines increase in size, it becomes more crucial to perform mass and load reduction techniques to obtain lighter structural members to help decrease the cost of energy. Reducing the blade weight and reaction forces at the hub is a natural place to

* Corresponding author. Tel.: +47-735-925-39; fax: +47-735-941-29.
E-mail address: kevin.cox@ntnu.no.

doi:10.1016/j.egypro.2013.07.153

start since reductions here allow for weight and cost savings throughout the other main structural components like the hub, shaft, and tower.

The method studied for load alleviation in this paper utilizes an adaptive blade with bend-twist coupling provided by an unbalanced glass/carbon hybrid composite layup. Many studies on this topic have been previously performed for various composite materials, regions of coupling on the blade, wind speeds, blade lengths, and design criteria [1] – [4].

A 9m blade was designed and manufactured in [1] in which carbon fibers were used in the airfoil skin to provide bend-twist coupling to an all fiberglass spar. At the extreme operating condition, the maximum tip twist achieved was 7.8°. The 33.25m adaptive blade created in [2] utilized an unbalanced layup also only in the blade skin regions and was capable of achieving a 4.1° tip twist due to a 12 m/s wind speed (with zero blade pitch). The parameter study in [3] considered various unbalanced layups in both the skin and spar of a 45m blade. A number of good results were achieved, but they are in terms of the effects on the turbine system (i.e. reductions in tower root moment), and are therefore difficult to compare with literature based at the turbine blade level. Another parameter study focused on finding the optimum fiber orientation to produce bend-twist coupling in a 37m blade with constraints on the percentage of unbalanced material allowed, material strengths, tip deflection and blade cost [4]. This study yielded results about which orientations were cheaper than others but did not provide any information about tip twist or load reduction. Similarly, twisting towards stall instead of feather (for fixed pitch turbines) has also been a topic of interest in [5], [6], though these results cannot be compared to variable pitch turbines because of the different maximum loading conditions.

Due to the nearly infinite number of design and load scenarios, it is difficult to understand from previous literature how the magnitude of the bend-twist coupling is affected by the blade size. Furthermore, most studies have been performed on blades for use in turbines rated below 3 MW. Therefore, there is motivation to determine how larger blades perform with bend-twist coupling, and moreover, how the coupling and load reductions scale with blade length.

1.1. Bend-twist coupling

Bend-twist coupling is unique to composite materials and has found a niche in aerodynamic structures for the possibility of tailoring the aerodynamic properties based on composite layup techniques and load application. This form of aerodynamic tailoring is passive in that no input is required for the structure to adapt; it adjusts based on changes in loads. The coupling stems from designing the structure with an unbalanced composite layup which imposes an inherent twisting deformation when bent about a certain axis. The amount of induced twist on the structure comes from utilizing the unbalanced layup and is also dependent on the structure's bending stiffness, torsional stiffness, length, and applied bending load. An equation developed by [7] suggests that for a constant cross-section beam, the amount of induced twist at the beam tip (φ_{tip}) is described by:

$$\varphi_{tip} = \frac{\alpha L^2 F}{2(1-\alpha^2)\sqrt{EIGJ}} \tag{1}$$

L is the length of the beam, F the applied bending load, EI the bending stiffness, GJ the torsional stiffness, and α the coupling coefficient. The parameter, α, exists between 1 and -1 where a value of 0 yields no coupling, and ± 1 yields the maximum with the sign indicating the direction of twist. In the case of turbine blades, the sign of α indicates whether the blade twists towards feather or stall. The magnitude of the coupling coefficient depends mainly on the difference between the fiber and matrix moduli, the fiber orientation, and the laminate stacking sequence. An equation for the coupling coefficient was also presented in [7] that describes the theoretical maximum amount of coupling; see equation (2).

$$\alpha = -\frac{\overline{D}_{16}}{\sqrt{\overline{D}_{11} * \overline{D}_{66}}} \quad (2)$$

Here, the D_{ij} components are those from the bending stiffness matrix and can be found in any book on mechanics of composite materials. The i and j subscripts refer to the global blade coordinate system with 1 pointing along the blade length, 2 (though not present in the equation) points in the blade chord direction and 6 represents the torsional component. The subscripts refer to the values at specific locations in the 3x3 stiffness matrix, where the i term corresponds to the stress in that direction and the j term describes the strain in its respective direction. D_{11} represents the composite's bending stiffness, D_{66} its torsional stiffness, and D_{16} represents the coupling stiffness between bending and twisting.

1.2. Up-scaling relations

When up-scaling a bend-twist coupled blade, it is of interest to predict how the induced twist will be affected by the change in size. It was possible to theoretically estimate the response of tip twist based on blade scaling by following the scaling laws presented below. First, the blade length was set as the independent variable, so the scaled length (L_s) was defined as in (3) and depended on the original length, L_n, and the scaling factor, f as in [8], [9]. The blade chord length and thickness were also linearly scaled as in (4) and (5), where C_n and T_n are the original chord length and thickness respectively.

$$L_s = fL_n \quad (3)$$

$$C_s = fC_n \quad (4)$$

$$T_s = fT_n \quad (5)$$

Implementing (3) – (5) into (6), the standard equation for aerodynamic lift, yielded the dependency of the flapwise bending load on the scaling factor, equation (7). This load is dependent on the air density (ρ), the area (A), the lift coefficient (C_L) and the square of the velocity. The velocity depends on both the rotational speed and wind speed but was assumed constant due to an assumed constant tip speed ratio as described in [9]. Therefore, for the scaling study in this project, all of the variables in (6) remained constant except for the area which scaled quadratically due to C_s and T_s.

$$F_n = \frac{1}{2}\rho A C_L V^2 \quad (6)$$

$$F_s = f^2 F_n \quad (7)$$

The authors continued this linear scaling technique to create scaling relations for the additional terms in (1), namely EI and GJ: the bending and torsional stiffnesses respectively. Assuming constant material properties, the bending and torsional stiffnesses were only dependent on the second moments of area of the blade cross-sections. This resulted in EI and GJ being proportional to the 4th power of the scaling factor as in (8) and (9).

$$EI_s = f^4 EI_n \quad (8)$$

$$GJ_s = f^4 GJ_n \quad (9)$$

Initial observation of (2) suggests that α depends on various laminate stiffnesses and therefore, the laminate thickness. However, all of the D_{ij}'s include equivalent thickness terms which can be canceled out of the equation. The coupling coefficient is therefore only dependent on the in-plane laminate properties (which were already assumed constant) and is therefore also assumed constant. Having

defined all variables in (1), the authors developed an equation to predict how the tip twist would scale with blade length. Rewriting (1) in terms of the scaling factor yielded (10).

$$\varphi_s = \frac{f^2 f^2}{\sqrt{f^4 f^4}} \varphi_n = \varphi_n \tag{10}$$

According to these scaling equations, there should be no change in induced twist from bend-twist coupling in up-scaled blades. In other words, the induced twist was predicted to be independent of geometric up-scaling. Experimental results from [7] also found that geometry had little effect on the magnitude of bend-twist coupling for a simple beam cross-section, composite layup and loading condition. However, many assumptions used in these equations may not hold for turbine blades:

- Blades do not have constant cross-sections along their spans
- The applied load changes along the length and provokes an aerodynamic twist-toward-stall moment
- A gravitational load exists
- Blades deform nonlinearly due to their slender structures
- Instabilities like buckling exist which bring on many other nonlinear issues
- The longitudinal and shear moduli, E and G, are not constant due to ply drops

Nonetheless, a theoretical linear up-scaling relation now existed and could be compared against the nonlinear finite element simulations performed in this study.

2. Design Methods

In order to study the effects of blade scaling on bend-twist coupling, well defined material properties, composite layups, and structural geometries were required. In addition, due to the slender shape of blades, nonlinear studies were required to accurately predict the response of a loaded blade. Due to the time consuming task of creating finite element models of blade designs, only 4 blade lengths have been chosen between 30 and 90 meters: representing typical blade lengths for multi-megawatt turbines (ranging from a 1.6 MW machine for the 30m blade to approximately 12-14 MW for the 90m blade).

2.1. Baseline blade designs

The 30, 50 and 90m blades were based off of a simplified scaling study presented in [10] while the 70m blade was that of the NOWITECH reference blade [11], [12] which is a much more refined design as will be discussed in the next sections. The geometries of each blade can be found in the above mentioned references, while the spanwise chord and thickness distributions are also shown in Figures 1 and 2.

The 70m blade utilized various airfoils along its span to obtain a balance between aerodynamic performance and structural rigidity. The 30, 50, and 90m blades (termed NACA-scaled blades or NSBs in this paper) were defined utilizing only the NACA 64(3)-618 airfoil along their entire spans. This airfoil is not typically used near the blade root due to its lower structural characteristics when compared to other airfoils. However, this was accounted for by using thick composite layups in this region to resist bending and buckling. When concerning mass, the NSBs may not be representative of other blades of similar length for this reason. However, despite these differences, the mass and stiffness near the blade root was found to have an insignificant contribution to bend-twist coupling as noted in [3], [13]. In fact, these studies showed negligible influence on the coupling even out to 30-35% of the blade span. The results of the present study also showed that this region had little effect on induced twist. The geometries of the NSBs were each individually created as a 3-dimensional shell surface in SolidWorks and imported to ABAQUS for FEA preprocessing.

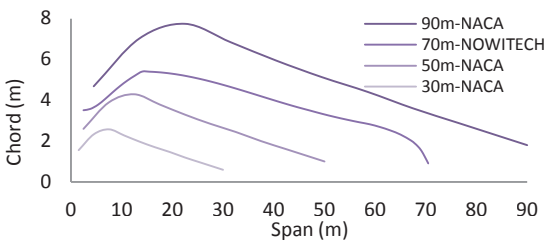

Figure 1: Spanwise chord length distribution of blades

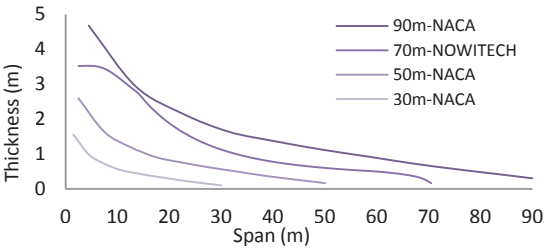

Figure 2: Spanwise thickness distribution of blades

They were then sectioned into 10 segments along the blade span to allow for load application points and localized ply layup specifications as in Figure 3. The 70m blade was designed in the same way but sectioned into 39 segments along the blade span as specified in [11], allowing for a more detailed ply layup and load distribution.

2.2. Blade loads

Each blade was fully fixed at the end where it would exit the hub connection. The S4R element in ABAQUS was used for the mesh of the NSBs and converged with 8 elements across the spar flanges, 5 on the webs, 6 on the upper and lower trailing regions, and 16 to create the leading edge as in Figure 4. This yielded 16172 nodes with 96768 degrees of freedom. The same mesh was used for the 30, 50, and 90m blades since the mesh scaled up exactly with the geometry. The 70m blade also used the S4R element as described in [11], but the mesh was finer than the NSBs due to the larger number of segments.

Aerodynamic loads were applied as point loads to the 4 vertices of the spar flange; the loads nearer the leading edge were weighted more heavily than those nearer the trailing edge to create the aerodynamic moment. The loads were applied according to the EWM (extreme wind speed model) load case: a 70 m/s gust incident on fully pitched blades with 15^{o} yaw error during parked (non-rotating) conditions as specified in [14]. This was found in [13] to be the worst case scenario for tip deflection on the 70m NOWITECH blade, and to isolate the effects of geometry on bend-twist coupling, this load case was used for all blades in this study.

The magnitudes of the loads at each section of the NSBs were found with (6): the lift coefficient being that of the NACA 64(3)-618 airfoil at each respective angle of attack along the blade length. The spanwise distribution of flapwise bending loads was equivalent for the NSBs with only the magnitude of each changing. Figure 5 shows the span-normalized load distribution for the NACA-scaled blades. Edgewise (drag) loads were not included due to their minor influence. A gravity load was also applied to each blade oriented in the vertical, pointing up position (3^{o} off the vertical axis to account for blade cone and shaft angle). Gravity contributed to flapwise bending from the slight off-axis blade orientation, and in addition, affected the critical buckling load due to the compressive force created by the blade's weight. The loads on the 70m blade followed the same procedure but were much more refined due to its 39 blade sections instead of 10 as in the NSBs. Details of the loads on the 70m blade are available in [11].

Figure 3: NACA-scaled blade geometry

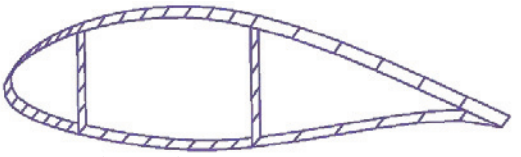

Figure 4: Blade mesh

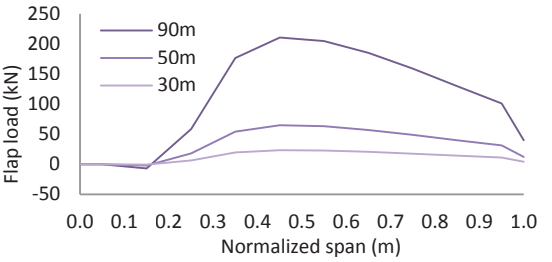

Figure 5: Flapwise load distribution on the NACA-scaled blades

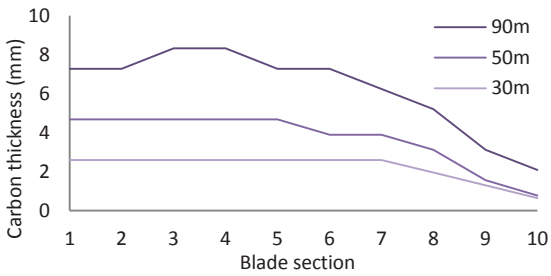

Figure 6: Carbon total thickness in spar flanges

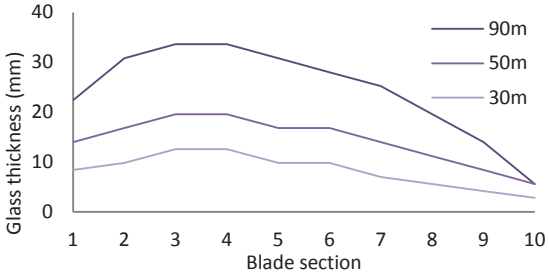

Figure 7: Biax ($\pm 45^o$) glass total thickness in spar flanges

2.3. Blade materials

The layup of each blade consisted of glass/carbon hybrid spar flanges (red regions in Figure 3) and glass and core material in the webs and leading and trailing regions. Carbon was oriented to 0^o (parallel to the pitch axis) in the spar flanges to provide bending stiffness, and biaxial ($\pm 45^o$) glass plies were used in all regions to provide torsional stiffness and resist buckling. The properties of the materials used in the NSBs are given in Table 1, while detailed information on the composite layup, material properties and safety factors of the 70m blade is provided in [11]. In Table 1, the last three columns specify the minimum ply thickness used for each blade length: 30m, 50m and 90m respectively. These thicknesses were based on integer values of the real ply thicknesses and were chosen to keep the total ply count down.

Table 1: Material Properties.

Material	E_{xx} GPa	E_{yy} GPa	Gxy GPa	υ_{xy} ---	ρ kg/m^3	e1c %	t-30 mm	t-50 mm	t-90 mm
0^o Carbon [15]	135.14	9.40	5.14	0.318	1580	-0.98	0.65	0.78	0.78
$\pm 45^o$, mat Glass [16]	13.60	13.30	10.35	0.490	1700	-1.80	1.40	2.80	2.80
Core [www.diab.com]	0.25	0.25	0.07	0.350	200	NA	3.00	3.00	5.00

For practicality, the baseline blades (and bend-twist coupled blades) were required to fulfill the design requirements specified in [14], [17]:

1. Minimum strain $\geq$ -0.330 in the carbon fibers.
2. Linear critical buckling load $\geq$ 2.04 (taken to be 2.0 to for simplicity).

The minimum strain value was based on reduction factors including the influence of aging and temperature, the layup technique, and a post-cured laminate applied to the characteristic strain value specified in Table 1. The critical buckling load safety factor came from a material safety factor, a temperature effect, and a linear finite element solution technique. Tip deflections and natural frequencies are also important design criteria but these were not considered as failure modes in this study, though their values were calculated and are presented in the results section.

The composite layups of each blade were determined individually through nonlinear quasi-static and linear buckling finite element simulations. If both design requirements were not achieved simultaneously, then material was added to the failed region of the blade and the simulations performed again. The resulting thickness distributions of carbon and glass plies in the spar flanges are shown in Figures 6 and 7 for the NSBs. The layups of the remaining structural regions of the blade were not as critical for this study and are therefore not presented.

2.4. *Applying bend-twist coupling*

After fully defining the baseline blades, the composite layups were modified to exhibit bend-twist coupling. For the NACA-scaled blades, this was done by rotation of the carbon fiber plies in the spar flanges to a 23^o off-axis orientation, while all other plies and regions of the blade were left unmodified.

This orientation was chosen because it produced the maximum α for the carbon fiber in Table 1. The adaptive 70m NOWITECH blade implemented a 20° off-axis carbon orientation as defined in *[13]*.

3. Results of Baseline Blades

The results are presented in Table 2. The mass of the blades was found to scale cubically with the blade length as is typical for such up-scaling studies. In addition, the tip deflection and the first flapwise frequency scaled linearly with increasing blade length, as expected. The 70m NOWITECH blade did not fit well with the curves predicted by the NACA-scaled blades for several reasons:

- Different airfoils and a different spanwise thickness distribution was used as seen in Figure 2.
- There were differences in material properties and material strengths
- Additional load cases were studied
- Nonlinear buckling studies were performed instead of linear (only 1.634 needed instead of 2.0 [17])
- More effort was put into mass reduction techniques than for the NACA-scaled blades

Table 2: Baseline blade results

Blade length	Mass (kg)	Carbon in flange % (mass)	Tip deflection (m)	1st flapwise freq. (Hz)	Buckling load
30m-NACA	2673.2	19.52	4.08	1.443	2.031
50m-NACA	11127.9	19.31	7.06	0.883	2.028
90m-NACA	70205.8	19.27	13.22	0.489	2.013
70m-NOWITECH	24929.4	35.37	4.78	0.698	1.659 (nonlinear)

4. Results of Adaptive Blades

The off-axis carbon fiber orientations decreased the bending stiffness as expected, and this required additional core material to be added in some of the trailing edge regions to resist buckling in the more compliant blade. The changes in blade stiffness, mass, tip deflection and resulting critical buckling load due to these changes were insignificant. The results of the coupled blades are shown in Table 3.

Table 3: Adaptive blade responses compared to baseline blades

Blade	Tip Twist (deg)	Tip Def (m)	1st Flap Freq (Hz)
30m-NACA	6.96	147.30 %	80.80 %
50m-NACA	5.84	147.50 %	81.20 %
90m-NACA	6.16	146.30 %	81.45 %
70m-NOWITECH	6.56	170.20 %	76.47 %

The maximum twist towards feather achieved for each blade existed at the tip; the magnitude was relatively constant and between about 6-7° for all blades. The composite layups were created with fixed glass and carbon ply thicknesses which resulted in step changes in thickness (and blade stiffness) and resulted in slightly over designed areas. For example, the design of the 30m blade may have needed only a 0.5mm increase in carbon thickness in a specific region, but a 0.65mm layer was placed since this was defined as the minimum ply thickness. Further refinement of the layups could be done, and it is likely that the tip twist for each of the NACA-scaled blades would approach a single value between 6 and 7°.

The induced twist of the 70m blade also existed in the range of the NSBs despite its design differences. Though exhibiting much lower deflection than the NSBs, it was able to achieve a similar maximum twist due to a higher percentage of off-axis carbon in the spar flanges (Table 2). However, this yielded a larger increase in tip deflection and decrease in the first flapwise natural frequency than in the NSBs.

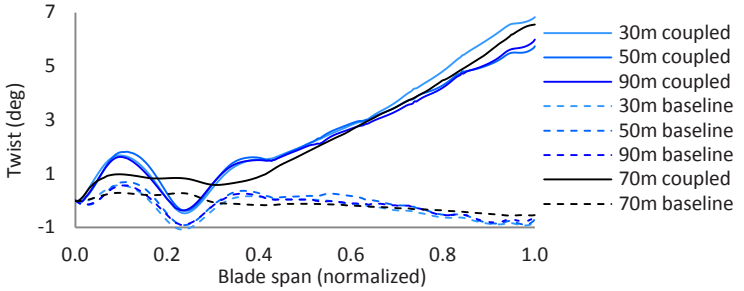

Figure 8: Spanwise twist distribution for baseline and coupled blades

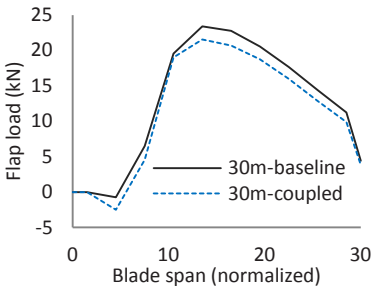

Figure 9: Load reduction of 30m blade

Figure 8 shows the spanwise twist induced for each blade and indicates minimal twisting achieved before approximately 30% span, concurring with [3], [13]. The sinusoidal shapes of the curves over the first 30% of span are due to the considerable changes in blade geometry in this region and exist even in the absence of bend-twist coupling as seen by the baseline curves in the figure. This was less significant in the 70m blade since it utilized a more torsionally stiff region near the root. Regardless of the nonlinearities in the blade stiffnesses and loading conditions, the same result has been achieved through the nonlinear FE study as in (10): that bend-twist coupling is independent of geometric up-scaling.

4.1. Non-operational aerodynamic load reduction

The resulting twist distributions from Figure 8 were added to the original baseline blade twist distributions and the bending loads recalculated for the EWM load condition. The reductions in flapwise loads were similar for each blade, with the spanwise distribution for the 30m blade shown in Figure 9 and the total reductions for all blades given in Table 4. The flap loads on the bend-twist coupled blades were between about 10 and 11 % lower than for the baseline blades and again seemed rather independent on blade size. The coupling yielded total bending moments that were about 9 to 10% lower than the baseline blades, though a slight decrease in reduction with increase in blade length was found (if the 70m results are ignored). Additional blades would need to be studied to verify if this comment is valid.

Table 4: Load and moment reductions from adaptive blades

Blade	% Reduction in Flap Load	% Reduction in Bending Moment
30m-NACA	10.84	10.01
50m-NACA	10.83	9.25
90m-NACA	9.93	8.68
70m-NOWITECH	10.42	10.48

4.2. Quasi-static effects on control system during operation

Further studies were performed on the 70m NOWITECH blade, subjecting it to various wind speeds with and without the pitch control system to study the development of bend-twist coupling through different operating regions of a wind turbine [13]. In addition, the studies determined the converged twist distribution of the blade instead of that after a single load iteration (as was done in the present study as shown in Figure 8). The converged twist distribution was again based on quasi-static simulations but was determined through an iterative procedure. In the converged calculation, the aerodynamic loads are recalculated for each stepwise change in induced twist. The induced twist changed based on the magnitude of the applied bending load. The flapwise bending loads that were input to the FE model yielded a bending-twisting response, creating a new twist distribution along the blade.

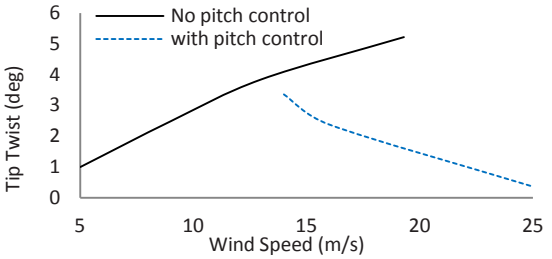

Figure 10: Tip twist versus wind speed

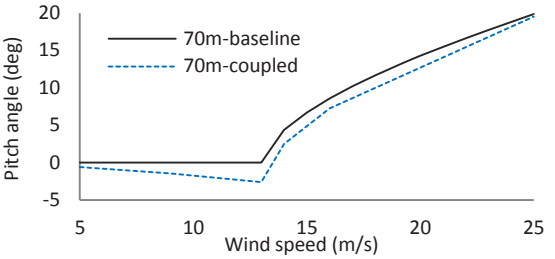

Figure 11: Control system pitch angle versus wind speed

New flapwise bending loads were then calculated with the aerodynamic program from [18] for this new twist distribution and applied to the original FE blade model; blade bending deformations were not accounted for during load recalculations. To find the accurate bending-twisting response, this procedure was repeated until the blade tip deflection, twist, and flapwise loads converged to within 1% of the solution. The maximum converged twist during the EWM for the 70m blade was found to be 6.00^o indicating a decrease of 8.5% from the single iteration study. Converged tip twist versus wind speed for turbine operational conditions is displayed in Figure 10.

The twist towards feather decreased the lift produced by the blade and yielded a reduction in the flapwise load and the Cp for all operating wind speeds. As it is undesirable to have a lower Cp than the baseline blade, a control system could be used to pitch the adaptive blade (towards stall) to an angle that would provide an equivalent Cp. This is shown graphically in Figure 11 which displays the full blade pitch angle needed to achieve equivalent Cp values for the 70m baseline and adaptive blades. The pitching scheme of Figure 11 matches well with those produced in [3]. Unfortunately, when pitching the blade back towards stall, the lift is increased again and therefore so are the flapwise loads and all load reduction capability is lost from the adaptive blade as discussed in [13]. The exception is for non-operational conditions (i.e. EWM) where the Cp is equal to zero but the flap loads are reduced (Table 4).

Due to the similar twist distributions achieved in the NACA-scaled blades for the EWM load case, it is likely that similar induced twist versus wind speed curves would be produced. In addition, similar control system pitch angles versus wind speed should be achieved as in the 70m NOWITECH blade.

A study performed on the 70m blade in [13] also found an increased critical buckling load due to the load reduction of the EWM case which allowed for removal of biax glass plies amounting to a 2.2% drop in blade mass. Further analysis of the NSBs would be required to confirm if the 2% mass reduction is transferrable between other blades achieving ~6^o of induced tip twist.

5. Conclusions

Blades of 30, 50, and 90m lengths were designed using a hybrid glass/carbon composite layup to determine the effects of blade scaling on bend-twist coupling. The carbon fiber plies were oriented to a 23^o off-axis orientation for these blades, while a 70m blade of a different design utilized an off-axis angle of 20^o. The coupled blades were subjected to a quasi-static load and allowed to deform nonlinearly. All blades yielded a maximum twist between about 6^o and 7^o indicating that up-scaling blade geometry has no effect on bend-twist coupling. This conclusion matched that predicted by the theoretical linear scaling equations. The induced spanwise twist distribution was also comparable between the blades and produced flapwise bending load reductions between about 10 and 11%. The 70m blade was subjected to further analysis to determine the dependency of tip twist on wind speed. A curve relating the control system pitch to wind speed was developed for the adaptive blade to achieve the same Cp as the baseline. Bend-twist coupling significantly reduced the maximum blade loads and moments while it also showed potential for blade mass reduction.

6. Further Work

Tip deflection and natural frequencies were not considered as failure modes in this study, but setting limits to these criteria would affect the allowable amount of bend-twist coupling. Shear strain failure and damage evolution would also be of interest to see their influence on the coupling and if they are dependent on geometric up-scaling. More blade designs and lengths should be considered to further confirm the results from this study. Finally, additional off-axis carbon fiber angles and modifications to the percentage of carbon fibers in the spar flanges could be studied to determine if bend-twist coupling remains to be independent of geometric up-scaling.

Acknowledgements

Thanks go to the Norwegian Research Centre for Offshore Wind Technology – NOWITECH – and to the Norwegian University of Science and Technology – NTNU – for funding this research and providing the tools and environment in which to conduct it; see htpp://www.nowitech.no.

References

[1] Berry D. Design of 9-meter Carbon-Fiberglass Prototype Blades: CX-100 and TX-100. Technical Report. Warren, RI: Sandia National Laboratories; 2007 TPI Composites, Inc. SAND2007-0201.
[2] Griffin D. Evaluation of Design Concepts for Adaptive Wind Turbine Blades. Technical Report. Albuquerque: Sandia National Laboratories; 2002 Global Energy Concepts, LLC. SAND2002-2424.
[3] Bottasso CL, Campagnolo F, Croce A, Tibaldi C. Optimization-Based Study of Bend-Twist Coupled Rotor Blades for Passive and Integrated Pasive/Active Load Alleviation. Technical Report. Milano: Politecnico di Milano; 2011. DIA-SR 11-02.
[4] Wetzel KW. Utility Scale Twist-Flap Coupled Blade Design. *Journal of Solar Energy Engineering*. 2005 November;127:529-537.
[5] Lobitz DW, Veers PS. Aeroelastic Behavior of Twist-Coupled HAWT Blades. Technical Report. Albuquerque: American Institute of Aeronautics and Astronautics; 1998 Sandia National Laboratories. AIAA-98-0029.
[6] de Goeij WC, van Tooren MJ, Beukers A. Implementation of bending-torsion coupling in the design of a wind-turbine rotor-blade. *Applied Energy*. 1999;63:191-207.
[7] Ong CH, Tsai SW. Design, Manufacture and Testing of A Bend-Twist D-spar. Technical Report. Stanford: Sandia National Laboratories; June 1999 Stanford University. SAND 99-1324.
[8] Manwell JF, McGowan JG, Rogers AL. Wind Turbine Design. In: *Wind Energy Explained*. Chichester (West Sussex): John Wiley & Sons Ltd; 2002.
[9] Griffith DT, Ashwill TD. The Sandia 100-meter All-glass Baseline Wind Turbine Blade: SNL100-00. Technical Report. Albuquerque: Sandia National Laboratories; 2011 Sandia National Laboratories. SAND2011-3779.
[10] TPI Composites, Inc. Parametric study for large wind turbine blades. WindPACT Blade System Design Studies. Technical Report. Warren, RI: Sandia National Laboratories; 2002 TPI Composites, Inc. SAND2002-2519.
[11] Cox K, Echtermeyer A. Structural Design and Analysis of a 10MW Wind Turbine Blade. *Energy Procedia*. 2012 August;24:194-201.
[12] Frøyd L, Dahlhaug O. Rotor Design for a 10 MW Offshore Wind Turbine. *The Proceedings of the Twenty-first (2011) International Offshore and Polar Engineering Conference*. 2011 June;1:327-334.
[13] Cox K, Echtermeyer A. Load alleviation from an adaptive 10 MW wind turbine blade. In: *DEWEK 2012, German Wind Energy Conference*; 2012; Bremen. Available from: http://www.dewi.de/DwK12pRocD/.
[14] IEC. Wind turbines - Part 1: Design Requirements. International Standard. Geneva: IEC 2005; 2005 International Electrotechnical Comission. IEC 61400-1 Third edition.
[15] Department of Defense. Composite Materials Handbook: Volume 3. Polymer Matrix Compoites Materials Usage, Design, and Analysis. Materials Handbook. Department of Defense; 2002. MIL-HDBK-17-3F.
[16] Mandell J, Samborsky D, Agastra P, Sears A. Analysis of SNL/MSU/DOE Fatigue Database Trends for Wind Turbine Blade Materials. Technical Report. Bozeman: Sandia National Laboratories; 2010 Montana State University. SAND2010-7052.
[17] Germanischer Lloyd. Guideline for the certification of wind turbines. International Standard. Hamburg 2010.
[18] Frøyd L, Dahlhaug OG. A Conceptual Design Method for Parametric Study of Blades for Offshore Wind Turbines. In: *Pro. of the ASME 2011 30th Int. Conf. on Ocean, Offshore and Arctic Engineering*; 2011; Rotterdam. p. 327-334.